
CONCLAD: COntinuous Novel CLAss Detector

Anonymous Author(s)

Affiliation

Address

email

Abstract

1 In the field of continual learning, relying on so-called oracles for novelty detection
2 is commonplace albeit unrealistic. This paper introduces CONCLAD ("COntinuous
3 Novel CLAss Detector"), a comprehensive solution to the under-explored problem
4 of continual novel class detection in post-deployment data. At each new task, our
5 approach employs an iterative uncertainty estimation algorithm to differentiate
6 between known and novel class(es) samples, and to further discriminate between the
7 different novel classes themselves. Samples predicted to be from a novel class with
8 high-confidence are automatically pseudo-labeled and used to update our model.
9 Simultaneously, a tiny supervision budget is used to iteratively query ambiguous
10 novel class predictions, which are also used during update. Evaluation across
11 multiple datasets, ablations and experimental settings demonstrate our method's
12 effectiveness at separating novel and old class samples continuously. We will
13 release our code upon acceptance.

14 1 Introduction and Related Work

15 Deployed AI models frequently encounter dynamic and evolving data distributions, where continuous
16 model adaptation is paramount to safeguard performance. Reliable novelty detection is a key
17 capability for adaptive AI. Novelty Detection will inform the model if there is new data and if so,
18 which samples are novel and need to be learnt from. However, until now, novelty detection and
19 continual adaptation have been tackled separately within different sub-fields of the AI scientific
20 literature. Most research in continual learning (CL) [1, 2, 3, 4, 5, 6] relies on fully labeled data,
21 despite the significant costs and impracticality of data labeling in real-world scenarios [7]. While
22 there are some unsupervised CL solutions [8, 9, 10], they often rely on an unrealistic assumption: that
23 for each new task and its incoming data, past classes do not appear alongside newly introduced classes,
24 thereby eliminating the need for novelty detection. Removing this oracle assumption results in severe
25 performance degradation due to overconfidence in erroneous predictions [11]: novel classes' samples
26 may be incorrectly predicted to old classes, especially at task transition onset where the continual
27 decision boundaries are still immature. Meanwhile, solutions for novelty or out-of-distribution (OOD)
28 detection [12, 13, 14, 15, 16, 17] have primarily been designed and evaluated using a single, fixed
29 split of old versus novel classes, rather than on continual splits. Additionally, conventional OOD
30 models often lack the ability to continuously integrate and learn from newly detected data. When
31 these models are forced to update, they can suffer from continual error propagation [11]: incorrect
32 novelty predictions during the detection stage lead to incorrect parameter learning during the update
33 stage, progressively degrading the overall system performance. The recently proposed incDFM
34 [11] offers an innovative solution to continual novel class detection (CND). However, incDFM was
35 designed for the simplistic scenario where only one novel class is introduced per task. This strong
36 assumption allows incDFM to treat all samples flagged as novel as members of the single new class,
37 enabling trivial pseudo-labeling for continual update. Due to this unrealistic one-class assumption,
38 incDFM cannot be considered fully unsupervised. In more complex cases with multiple novel classes,
39 incDFM fails to function effectively since it cannot distinguish between different novel classes.
40 In effect, all samples from those multiple novel classes are erroneously assigned to a single new
41 class. This multi-class "collapse" results in a poor estimate of the OOD/novelty distribution and
42 consequently, poor performance. Generalizing to the scenario of continuous multi-class novelties is
43 challenging, necessitating the creation of entirely new algorithmic components. **Our contribution is**

44 **as follows:** We propose CONCLAD (COntinuous Novel CLAss Detector), an iterative multi-class
 45 uncertainty estimation algorithm designed for generalized Continual Novelty Detection. We utilize
 46 the uncertainty scores to select (a) a very small fraction (0.3% - 1.25%) of samples from the unlabeled
 47 pool for supervision and (b) a suitable subset of the remaining unlabeled samples for automatic
 48 (unsupervised) pseudo-labeling. Through experimentation on various continual tasks and datasets,
 49 we demonstrate that CONCLAD excels in continually identifying the presence of (up to multiple)
 50 novel classes and accurately separating novel class samples from old ones.

51 2 Our Method

52 **2.1. Problem Setting:** Consider a continual agent $A(x, t)$ which needs to learn/adapt from a set of
 53 continual tasks. At each task t , $A(x, t)$ is presented with an initially unlabeled set of samples $U(t)$
 54 which consists in a mixture of unseen samples of its old/learned classes $U_{old}(t)$ and unseen samples of
 55 new (novel) classes $U_{new}(t)$:

$$U(t) = U_{old}(t) \cup U_{new}(t), \text{ where } U_{old}(t) = \{x|x \sim \bigcup_{k=1}^{t-1} D_k\}, U_{new}(t) = \{x|x \sim D_t\}, \quad (1)$$

56 Here D_t comprises samples from the set of new classes C_{new}^t introduced at task t , while $\bigcup_{k=1}^{t-1} D_k$
 57 are samples belonging to all the old classes C_{old}^t that have been learned up to and including task $t - 1$.
 58 Samples in $U_{old}(t)$ are “unseen”, meaning they were never used, neither in the initial training nor
 59 during prior tasks’ learning. Note that addressing data drifts in U_{old} is beyond the scope of this work.

60 **2.2. Our solution:** We introduce a continual novelty detector $N(x, t)$, operating alongside the
 61 continual agent, whose goal is to produce a reliable estimate of novel samples $\hat{U}_{new}(t)$ while
 62 simultaneously estimating their respective novel-class labels. Simply performing a binary distinction
 63 between novel-class and old-class samples (as in incDFM[11]) leads to poor results in novel multi-
 64 class settings. Moreover, the dependence on task index t in $N(x, t)$ indicates that the novelty detector
 65 itself has to be continually updated so that novel classes at t are not considered novel at $t + 1$. To
 66 obtain novel-class labels in $\hat{U}_{new}(t)$, one can either use unsupervised clustering methods [18], or
 67 active supervision (i.e. labeling by an expert) [19, 20, 21]. Here, we share initial results using active
 68 supervision for a tiny fraction of $U(t)$ (0.3% - 2.5%), along with pseudo-labeling of confidently
 69 identified novel samples in $\hat{U}_{new}(t)$. For all these tasks – novelty detection, sample selection for active
 70 labeling, and for pseudo-labeling – $N(x, t)$ relies foundationally on a novel, iterative multi-class
 71 uncertainty estimation method 2 defined and explained in the next sections.

72 **2.2.1. Building block of CONCLAD’s uncertainty formulation $S(i)$:** CONCLAD’s uncertainty
 73 estimation 2 uses the *feature reconstruction error* (FRE) [14], which is effective in novelty estimation
 74 for the closed-world and the single-class increment CL [11]. FRE involves learning a PCA transform
 75 \mathcal{T}_m and its inverse \mathcal{T}_m^\dagger for each class m . A test feature $u = g(x)$ is transformed by \mathcal{T}_m and re-
 76 projected back using \mathcal{T}_m^\dagger , with FRE calculated as the ℓ_2 norm of the difference between the original
 77 and reconstructed vectors. High FRE scores indicate samples that don’t belong to class m . In the
 78 simplified single-class increment CL [11], a single PCA transform is used for all ID data.

79 **2.2.2. Step by Step Novelty Detection:** Prior to deployment (task $t = 0$), we assume that an
 80 agent $A(x, t = 0)$ has been trained to classify among a fixed set of pre-deployment classes C_{new}^0 .
 81 Accordingly, CONCLAD’s novelty detector $N(x, t = 0)$ has been trained to recognize those classes
 82 as learned/old by having computed FRE transforms for those classes, $\mathcal{T}_m, \forall m \in C_{new}^0$. For a given
 83 future task $t > 0$, as unlabeled data arrives, $N^{(i)}(x, t)$ follows an iterative procedure (indexed by an
 84 inner-loop index, i , which is distinct from outer-loop task-index t) to learn to detect if/what novelties
 85 are present. At the first inner iteration $i = 0$, initial supervision querying is performed by picking
 86 samples (subject to labeling budget) with high uncertainty scores w.r.t old classes defined as $S^0(u) \triangleq$
 87 $\min_{j \in C_{old}^t} FRE_j^0(u)$. b_0 is sampled uniformly among samples with $S^0(u) > \text{mean}(S^0(u))$. At this
 88 point, novel classes can be identified (denoted by $|C_{new}^t|$ in section 2.1, assuming $|C_{new}^t| > 0$) and
 89 those few labeled samples are used to initialize parameters of $N^{(0)}(x, t)$: (1) Train a single layer
 90 perceptron, $N_{pl}^{(i)}(x, t)$ to learn an imperfect initial mapping to the $|C_{new}^t|$ novel classes. This layer,
 91 which performs pseudo-labeling (pl), contains output nodes only w.r.t novel classes. (2) compute
 92 rough estimates of per-novel-class PCA transforms $\{\mathcal{T}_m^{t,0}\}, m \in C_{new}^t$. Note that it’s possible that
 93 not all true novel classes are found in this initial iteration and may be found in subsequent ones. For
 94 subsequent iterations $i > 0$, given an unlabeled sample $x \in U(t)$, $N_{pl}^{(i)}(x, t)$ predicts a pseudo-label
 95 $m, m \in C_{new}^t$ which then routes the selection of the corresponding PCA transform $\mathcal{T}_m^{t,i-1}$ resulting

96 in the $i^{text{th}}$ iteration’s uncertainty score $S^i(x)$ 2:

$$S^i(u) = \min_{j \in C_{old}^t} \frac{FRE_j^0(x)}{FRE_m^{i-1}(x)}; i > 0, m = N_{pl}^{(i)}(x, t) \in C_t^{new} \quad (2)$$

97 $S^i(x)$ can be used to robustly categorize samples in $U(t)$ as: **(1) Novel with high-confidence:** These
 98 are samples with the highest score values (high numerator relative to the denominator). A high
 99 value of numerator implies large distance from previously seen classes C_{old}^t , while a low value of
 100 the denominator implies low distance from novel class m . Such a sample likely belongs to $U_{new}(t)$
 101 and is a strong candidate to be pseudo-labeled. From these, we select the topmost most confident α
 102 percent to pseudo-label. **(2) Old-class with high-confidence:** lowest score values corresponding
 103 to low numerator (low distance w.r.t C_{old}^{t-1}) and high denominator value (high-distance from the
 104 predicted novel class m). Such a sample likely belongs to $U_{old}(t)$, i.e. to an old class that has
 105 already been learned; **(3) Ambiguous:** Samples for which the score is neither definitively high nor
 106 definitively low. These could be old-class samples having relatively high scores, or new-class samples
 107 having relatively low scores. Owing to this ambiguity, a clear determination cannot be made. Hence,
 108 these samples are excellent candidates for active querying to minimize novelty detection uncertainty.
 109 At each inner-loop iteration, accumulated active and pseudo-labeled samples are used to re-update
 110 $N^{(i+1)}(x, t)$ ’s parameters (pseudo-labeler $N_{ps}^{(i)}(x, t)$, and FRE transforms $\mathcal{T}_m^{t, i-1}$). At the end of
 111 the inner-loop, all accumulated active and pseudo labeled samples are used to compute final PCA
 112 transforms $\{\mathcal{T}_m^t\}$ for $m \in C_t^{new}$ to permanently update the novelty detector $N(x, t)$ so those classes
 113 are not flagged as novel subsequently. Note that the pseudo-labeler, since it maps only to a given tasks
 114 detected novel classes, will be re-initialized at another tasks’ onset. Further methodology details,
 115 including inner-loop stopping criteria and ambiguity formulation, can be found in appendix sections.

116 3 Experiments

117 **3.1. Setup:** We evaluate on 4 datasets: Imagenet21K-OOD (Im21K-OOD) [22], Eurosat [23],
 118 iNaturalist-Plants-20 (Plants) [24] and Cifar100-superclasses [25], all of which were constructed to
 119 have no class overlap with Imagenet1K with the exception of Cifar100. Results for Cifar100 are
 120 included to enable direct comparison with baseline method incDFM [11]. We compare CONCLAD to:
 121 (1) incDFM [11], which first introduced an updatable continual novelty detector, albeit exclusively for
 122 single class novelties (see section 1); (2) DFM [26], originally proposed for static novelty detection.
 123 We also include semi-supervised CND baselines: (3) Experience-Replay "ER" [27, 6] uses entropy
 124 as a measure of novelty similar to [28] and also to select active labels; (3) PseudoER [29], same as
 125 ER, but iteratively pseudo-labels the most confident samples akin to CONCLAD. Other baselines
 126 are constructed (Fig 2 right table) from removing elements of CONCLAD such as the iterativeness
 127 (i.e. doing AL/Pseudo-labeling in one shot), etc. Implementations for CONCLAD and baselines: All
 128 use a large/foundation frozen feature extractor, e.g. ResNet50 [30] pre-trained on ImageNet1K via
 129 SwAV [31] or ViTs16 [32] pre-trained on Imagenet1K via DINO [33]. CONCLAD’s A_s^{cl} (pseudo-
 130 labeling head) is a fully connected layer. Baselines ER, PseudoER’s long-term classification head
 131 is a perceptron of size 4096. For ER and PseudoER we use a fixed replay buffer size containing
 132 pre-logit deep-embeddings and labels/pseudo-labels. We set the maximum buffer size to 5000 (2500
 133 for Eurosat). At each incoming unlabeled pool, we fix a mixing ratio of 2:1 of old to new classes
 134 per task, with old classes drawn from a holdout set (0.35% of each dataset). For evaluation on the
 135 independent test set, we sample old and new classes with the same 2:1 proportion. Note that old
 136 classes act as distractors from the point of view of novelty detection. We set pseudo-labeling selection
 137 to $\alpha = 20\%$ of samples predicted as novel (appendix 4.1.1). For experiments not purposely varying
 138 the tiny supervision budget, we fix a labeling budget of 1.25% for Places, Plants and 0.625% for
 139 Eurosat, Im21K-OOD, as guided by Fig 1 center which varies the AL budget from 0.625% to 5%.

140 **3.2. Results:** We measure continual novelty detection performance with the common "Area Under
 141 the Receiver-Operating-Curve" (AUROC) metric. Note that, for fair evaluation, we measure CND
 142 on an independent test set with the same ratio of old to new class samples at each task. Fig. 1
 143 (left) displays CND performance (AUROC) over all continual tasks (time) in the case of multi-
 144 class novelties per task (5 class increments for Im21K-OOD and 2 class increment for Eurosat).
 145 Additionally, figure X (center) shows the sensitivity of CONCLAD and other actively-supervised
 146 baselines (ER-entropy, PseudoER-entropy, section 3.1) when varying the tiny supervision budget
 147 (tested for a range of 0.32% to 5% of the unlabeled train data at each task). Fig. 1 (right) shows the
 148 effect of varying the novel class increment per task as measured by the AUROC score averaged over
 149 all continual tasks (with that given increment). Some interesting highlights: (1) we can see in Fig 1

150 (right) that the compared approach incDFM [11] performs reasonably well for the increment of only
 151 one novel class per task, for which it was originally proposed and tested by the authors. However,
 152 when the class increment increases, this method degrades in performance because it groups multiple
 153 novel classes with no distinction, which hurts detection. (2) PseudoER consistently under-performs
 154 ER because it is unable to produce high confidence pseudo-labels to be used in training and this in
 155 turn degrades its performance - this highlights the importance of our uncertainty metric 2 in measuring
 156 pseudo-label confidence. (3) It is evident in the above plots that even with tiny supervision budgets
 157 (e.g. 0.32%-1.25%), CONCLAD consistently outperforms the competing methods by a large margin
 158 over the several experimental variations.

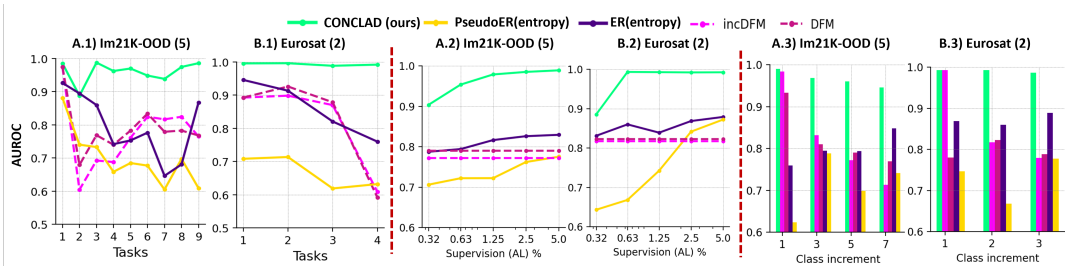


Figure 1: (Left A.1,B.1) Continual Novelty Detection performance measured by AUROC at each task. The number of novel classes introduced per task is in parenthesis. Overall, CONCLAD (green) significantly over-performs baselines; (Center A.2,B.2) Results varying the supervision budget; (Right A.3,B.3) Results varying Novel Class Increment per task. For (left,right) Supervision budget is 0.625% for CONCLAD, ER, PseudoER. Equivalent plots for Cifar100, Plants in appendix 4.3.

	Im21K		Plants		Eurosat		Cifar100		Variations (R50)	Im21K	Plants	Eurosat	Cifar100
	R50	ViT	R50	ViT	R50	ViT	R50	ViT					
CONCLAD(ours)	96.0	88.0	73.6	58.8	99.3	82.3	80.6	83.3	Default	96.0	73.6	99.3	80.6
incDFM	77.3	76.0	68.7	58.2	81.8	74.9	66.3	66.3	Sup-Top	89.5	71.0	97.6	81.9
DFM	79.0	75.4	67.4	54.9	82.2	74.9	62.2	66.3	Sup-Rand	88.7	65.9	98.9	80.4
ER-Entropy	79.4	52.8	61.4	52.4	86.0	46.6	64.1	55.4	No-Iters	89.5	68.2	80.5	66.4
PseudoER-Entropy	69.9	54.2	60.6	52.5	66.8	46.5	59.5	52.6	No-Pseudo	77.2	65.4	75.6	64.1

Figure 2: (Left) Continual Novelty Detection measured by AUROC; (Right) Ablations of CONCLAD. Supervision budget is 0.625% for Im21K, Eurosat and 1.25% for Plants, Cifar100

159 Fig 2 table (left) shows average AUROC results over all tasks for all 4 datasets and with two different
 160 feature extraction backbones (Vision Transformer "ViT" and Resnet50 "R50" described in section 3.1).
 161 In sum, similar conclusions can be reached here: CONCLAD significantly overperforms baselines
 162 over all the tested settings. Additionally, Fig 2 table (right) shows results for different ablations of
 163 CONCLAD: (*No-Pseudo*) Removing Pseudo-labeling from $S(i)$, i.e. computing per-novel class PCAs
 164 only with ground-truth label assignments obtained with the tiny labeling budget; (*Sup-Random*) Using
 165 random sampling to query ground truth labels with the same tiny budget; (*Sup-Top*) queries samples
 166 with highest uncertainty scores (i.e. most-confidently novel samples) for ground-truth labeling rather
 167 than ambiguous samples; (*No-Iters*) CONCLAD in oneshot. Use all supervision budget upfront and
 168 then pseudo-label in one-shot. The ablation results highlight the importance of minimizing error
 169 propagation via our method's iterativeness since No-Iters results in an average 11.2% decrease in
 170 performance. Similarly, we show that pseudo-labeling among the multiple novel classes detected is
 171 fundamental to performance given the AL budget's tiny size: No-Pseudo results in 16.8% average
 172 decrease. Finally, other active labeling strategies (i.e. Sup-Top) or lack thereof (Sup-Rand) also
 173 decrease performance by 2.4% and 3.9% respectively, underscoring the informativeness of querying
 174 ambiguous samples for AL with the goal of continual novelty detection, refer to section 2.2.2.

175 **Key Takeaways:** In this work, we presented CONCLAD, a solution to the still under-explored
 176 problem of continual novelty detection (CND). Our method enables CND in the generalized set-
 177 ting of novelties containing up to multiple novel classes. To achieve this, CONCLAD includes a
 178 foundationally novel iterative multi-class uncertainty estimation procedure capable of effectively
 179 modelling the distribution of multiclass novelties, only with a tiny supervision budget. By minimizing
 180 the number of samples falsely flagged as novel or overlooked as old, we ensure minimal continual
 181 error propagation. Overall, CONCLAD outperforms baselines over multiple large-scale datasets and
 182 experimental variations. Yet, several challenges remain for CND, which we hope to address in future
 183 work. One nontrivial example is how to detect both novel classes and distribution shifts of old classes
 184 (e.g. noise, illumination, etc) together, with minimal to no supervision.

References

- 185
- 186 [1] James Kirkpatrick et al. “Overcoming catastrophic forgetting in neural networks”. In: *Proceed-*
187 *ings of the national academy of sciences* 114.13 (2017), pp. 3521–3526.
- 188 [2] Shixian Wen et al. “Beneficial Perturbation Network for designing general adaptive artificial
189 intelligence systems”. In: *IEEE Transactions on Neural Networks and Learning Systems*
190 (2021).
- 191 [3] Brian Cheung et al. “Superposition of many models into one”. In: *Advances in neural informa-*
192 *tion processing systems* 32 (2019).
- 193 [4] Sylvestre-Alvise Rebuffi et al. “icarl: Incremental classifier and representation learning”. In:
194 *Proceedings of the IEEE conference on Computer Vision and Pattern Recognition*. 2017,
195 pp. 2001–2010.
- 196 [5] Amanda Rios and Laurent Itti. “Lifelong Learning Without a Task Oracle”. In: *2020 IEEE*
197 *32nd International Conference on Tools with Artificial Intelligence (ICTAI)*. IEEE. 2020,
198 pp. 255–263.
- 199 [6] Pietro Buzzega et al. “Rethinking experience replay: a bag of tricks for continual learning”. In:
200 *2020 25th International Conference on Pattern Recognition (ICPR)*. IEEE. 2021, pp. 2180–
201 2187.
- 202 [7] German I Parisi et al. “Continual lifelong learning with neural networks: A review”. In: *Neural*
203 *Networks* 113 (2019), pp. 54–71.
- 204 [8] Zhiqi Kang et al. “A soft nearest-neighbor framework for continual semi-supervised learn-
- 205 ing”. In: *Proceedings of the IEEE/CVF International Conference on Computer Vision*. 2023,
206 pp. 11868–11877.
- 207 [9] Matteo Boschini et al. “Continual semi-supervised learning through contrastive interpolation
208 consistency”. In: *Pattern Recognition Letters* 162 (Oct. 2022), pp. 9–14. ISSN: 0167-8655. DOI:
209 10.1016/j.patrec.2022.08.006. URL: [http://dx.doi.org/10.1016/j.patrec.](http://dx.doi.org/10.1016/j.patrec.2022.08.006)
210 2022.08.006.
- 211 [10] Benedikt Bagus, Alexander Gepperth, and Timothée Lesort. *Beyond Supervised Continual*
212 *Learning: a Review*. 2022. arXiv: 2208.14307 [cs.LG].
- 213 [11] Amanda Rios et al. “incdfm: Incremental deep feature modeling for continual novelty detec-
- 214 tion”. In: *European Conference on Computer Vision*. Springer. 2022, pp. 588–604.
- 215 [12] Dan Hendrycks and Kevin Gimpel. “A baseline for detecting misclassified and out-of-
- 216 distribution examples in neural networks”. In: (2017).
- 217 [13] Shiyu Liang, Yixuan Li, and R Srikant. “Enhancing the reliability of out-of-distribution image
218 detection in neural networks”. In: (2018).
- 219 [14] Ibrahima Ndiour, Nilesh A Ahuja, and Omesh Tickoo. “Out-Of-Distribution Detection
220 With Subspace Techniques And Probabilistic Modeling Of Features”. In: *arXiv preprint*
221 *arXiv:2012.04250* (2020).
- 222 [15] Kimin Lee et al. “A simple unified framework for detecting out-of-distribution samples and
223 adversarial attacks”. In: *Advances in Neural Information Processing Systems*. 2018, pp. 7167–
224 7177.
- 225 [16] Haoqi Wang et al. “ViM: Out-Of-Distribution with Virtual-logit Matching”. In: *Proceedings of*
226 *the IEEE/CVF Conference on Computer Vision and Pattern Recognition*. 2022.
- 227 [17] Jie Ren et al. “Likelihood ratios for out-of-distribution detection”. In: *Advances in Neural*
228 *Information Processing Systems*. 2019, pp. 14707–14718.
- 229 [18] Yazhou Ren et al. “Deep clustering: A comprehensive survey”. In: *IEEE Transactions on*
230 *Neural Networks and Learning Systems* (2024).
- 231 [19] Vu-Linh Nguyen, Mohammad Hossein Shaker, and Eyke Hüllermeier. “How to measure
232 uncertainty in uncertainty sampling for active learning”. In: *Machine Learning* 111.1 (2022),
233 pp. 89–122.
- 234 [20] Yarin Gal, Riashat Islam, and Zoubin Ghahramani. “Deep bayesian active learning with image
235 data”. In: *International Conference on Machine Learning*. PMLR. 2017, pp. 1183–1192.
- 236 [21] Donggeun Yoo and In So Kweon. “Learning loss for active learning”. In: *Proceedings of the*
237 *IEEE/CVF Conference on Computer Vision and Pattern Recognition*. 2019, pp. 93–102.
- 238 [22] Tal Ridnik et al. *ImageNet-21K Pretraining for the Masses*. 2021. arXiv: 2104.10972
239 [cs.CV].

- 240 [23] Patrick Helber et al. *EuroSAT: A Novel Dataset and Deep Learning Benchmark for Land Use*
241 *and Land Cover Classification*. 2019. arXiv: 1709.00029 [cs.CV].
- 242 [24] Grant Van Horn et al. *The iNaturalist Species Classification and Detection Dataset*. 2018.
243 arXiv: 1707.06642 [cs.CV].
- 244 [25] Alex Krizhevsky. “Learning Multiple Layers of Features from Tiny Images”. In: *University of*
245 *Toronto* (May 2012).
- 246 [26] Ibrahima J Ndiour, Nilesh A Ahuja, and Omesh Tickoo. “Subspace Modeling for Fast Out-
247 Of-Distribution and Anomaly Detection”. In: *2022 IEEE International Conference on Image*
248 *Processing (ICIP)*. IEEE, 2022, pp. 3041–3045.
- 249 [27] David Rolnick et al. “Experience replay for continual learning”. In: *Advances in Neural*
250 *Information Processing Systems* 32 (2019).
- 251 [28] Rahaf Aljundi et al. “Continual novelty detection”. In: *Conference on Lifelong Learning*
252 *Agents*. PMLR, 2022, pp. 1004–1025.
- 253 [29] Dong-Hyun Lee. “Pseudo-Label : The Simple and Efficient Semi-Supervised Learning Method
254 for Deep Neural Networks”. In: *ICML 2013 Workshop : Challenges in Representation Learning*
255 *(WREPL)* (July 2013).
- 256 [30] Kaiming He et al. “Deep residual learning for image recognition”. In: *Proceedings of the IEEE*
257 *conference on computer vision and pattern recognition*. 2016, pp. 770–778.
- 258 [31] Mathilde Caron et al. “Unsupervised learning of visual features by contrasting cluster as-
259 signments”. In: *Advances in Neural Information Processing Systems* 33 (2020), pp. 9912–
260 9924.
- 261 [32] Dosovitskiy Alexey. “An image is worth 16x16 words: Transformers for image recognition at
262 scale”. In: *arXiv preprint arXiv: 2010.11929* (2020).
- 263 [33] Mathilde Caron et al. “Emerging properties in self-supervised vision transformers”. In: *Pro-*
264 *ceedings of the IEEE/CVF international conference on computer vision*. 2021, pp. 9650–
265 9660.
- 266 [34] Yen-Chang Hsu et al. “Generalized odin: Detecting out-of-distribution image without learning
267 from out-of-distribution data”. In: *Proceedings of the IEEE/CVF Conference on Computer*
268 *Vision and Pattern Recognition*. 2020, pp. 10951–10960.
- 269 [35] Utku Evci et al. “Head2toe: Utilizing intermediate representations for better transfer learning”.
270 In: *International Conference on Machine Learning*. PMLR, 2022, pp. 6009–6033.
- 271 [36] Alexander A Petrov, Barbara Anne Doshier, and Zhong-Lin Lu. “The dynamics of perceptual
272 learning: an incremental reweighting model.” In: *Psychological review* 112.4 (2005), p. 715.
- 273 [37] Guneet S Dhillon et al. “A baseline for few-shot image classification”. In: *arXiv preprint*
274 *arXiv:1909.02729* (2019).
- 275 [38] Diederik P Kingma and Jimmy Ba. “Adam: A method for stochastic optimization”. In: *arXiv*
276 *preprint arXiv:1412.6980* (2014).
- 277 [39] Amanda Rios and Laurent Itti. “Closed-loop memory GAN for continual learning”. In: *arXiv*
278 *preprint arXiv:1811.01146* (2018).
- 279 [40] Olga Russakovsky et al. “ImageNet Large Scale Visual Recognition Challenge”. English
280 (US). In: *International Journal of Computer Vision* 115.3 (Dec. 2015). Publisher Copyright:
281 © 2015, Springer Science+Business Media New York., pp. 211–252. ISSN: 0920-5691. DOI:
282 10.1007/s11263-015-0816-y.
- 283 [41] Pengzhen Ren et al. “A survey of deep active learning”. In: *ACM computing surveys (CSUR)*
284 54.9 (2021), pp. 1–40.

285 4 Appendix

286 4.1 Methodology Details

287 4.1.1 Thresholds for Stopping the inner-loop

288 The inner-loop is guided by two simple thresholds: (1) Threshold T_{inner} "roughly" estimates if
289 there are any possible novel-class samples in the unlabeled task input data pool and is controlled by
290 a single hyper-parameter, the number of standard deviations above the mean of an in-distribution
291 validation set (2 STDs in our experiments). If no samples are found to be above T_{inner} , we reach the

292 stopping criterion for our iterations. Our in-distribution validation set is conventionally defined to
 293 include a portion (0.1%) of the previous tasks’ $k = 1 : t - 1$ novelty predictions that were held-out
 294 at previous tasks, i.e. not used to update $N(x, t)$ parameters. Importantly, the same in-distribution
 295 validation set is used for all compared baselines in our results section, as is common practice in the
 296 OOD/novelty-detection literature [11, 34]; (2) Finally, Threshold α tunes pseudo-labeling selection
 297 and is set to $\alpha = 20\%$ highest $S^i(u)$ scores (most confident) from the test samples found above
 298 T_{inner} . These two thresholds are not highly sensitive.

299 4.1.2 How to define Ambiguity

300 CONCLAD seeks to minimize novelty-detection uncertainty and model multiclass-novelty by
 301 selecting the most novel-vs-old ambiguous samples at each inner-loop iteration, i.e. scores $S^i(u)$
 302 which are neither too high or too low. Our mathematical formulation uses the threshold T_{inner} defined
 303 in the previous section: we formulate ambiguousness as the inverse squared distance $\frac{1}{\|S^i(u) - T_{inner}\|^2}$
 304 of scores to T_{inner} . Intuitively, this formula favors selecting samples that cannot be unambiguously
 305 predicted as either old or new since T_{inner} represents this rough decision boundary. Active selection
 306 is stopped when the tiny labelling budget is exhausted. The only exception to this Ambiguity
 307 formulation is at the first iteration $i = 0$ where we select homogeneously from samples above
 308 T_{inner} . This is the case because at $i = 0$ only old classes are used to compute the score function,
 309 $S^0(u) = \min_{j \in C_{old}^t} FRE_j^0(u)$ and so ambiguity cannot be defined in the same way as for the
 310 remainder of iterations.

311 4.1.3 Measuring per-class uncertainty in CONCLAD’s $S^i(u)$ formulation

312 CONCLAD is agnostic to the elemental uncertainty metric used in its uncertainty scoring function
 313 ($S^i(u)$ Eq. 2 in section 2) as long as it can reliably estimate uncertainty w.r.t each novel class or old
 314 class. However, this is not an easy feat since many existing static uncertainty quantification approaches
 315 are not fully reliable [14, 11]. As discussed in the main text, CONCLAD currently leverages the
 316 *feature reconstruction error* (FRE) metric introduced in [14] to build Eq 2. For each in-distribution
 317 class, FRE learns a PCA (principal component analysis) transform $\{\mathcal{T}_m\}$ that maps high-dimensional
 318 features u from a pre-trained deep-neural-network backbone $g(x)$ onto lower-dimensional subspaces.
 319 During inference, a test-feature $u = g(x)$ is first transformed into a lower-dimensional subspace by
 320 applying \mathcal{T}_m and then re-projected back into the original higher dimensional space via the inverse \mathcal{T}_m^\dagger .
 321 The FRE measure is calculated as the ℓ_2 norm of the difference between the original and reconstructed
 322 vectors:

$$FRE_m(u) = \|f(x) - (\mathcal{T}_m^\dagger \circ \mathcal{T}_m)u\|_2. \quad (3)$$

323 Intuitively, FRE_m measures the distance of a test-feature to the distribution of features from class m .
 324 If a sample does not belong to the same distribution as that m th class, it will usually result in a large
 325 reconstruction score FRE_m . FRE is particularly well suited for the continual setting since for each
 326 new class discovered at test-time, an additional principle component analysis (PCA) transform can be
 327 trained without disturbing the ones learnt for previous classes.

328 4.2 Experimental Methodology Details

329 4.2.1 Implementation Details for CONCLAD and Baselines

330 $N(x, t)$ operates on top of a large-scale/foundation models as feature extraction backbones, kept
 331 frozen throughout CONCLAD and baselines’ training: (1) Most results use ResNet50 [30] unsupervis-
 332 edly pre-trained on ImageNet1K via SwAV [31]. We extract features from the pre-logit AvgPool layer
 333 of size 2048 as deep-embeddings. We also experimented with other feature extraction points [14] but
 334 those under-performed w.r.t the pre-logit layer. (2) We also show results using ViTs16 [32] pretrained
 335 on Imagenet1K via DINO [33]. For ViTs16 we tried several extraction points, e.g. head, last norm
 336 later, different transformer block outputs with different pool factors (e.g. 2,4). Best results were
 337 obtained with the norm layer. Note that learning on frozen deep features is commonplace in vision
 338 CL and domain-adaptation fields [5, 11, 35]. It is theoretically based on the principle that low-level
 339 visual features from a large-scale/foundation frozen model are task nonspecific and do not need
 340 to be constantly re-learned. Rather, learning may happen upstream by utilizing the extracted deep
 341 features (at the last or inner-layers, or a combination thereof - an active research area) [36, 37, 35].
 342 CONCLAD’s $N(x, t)$ fully-connected pseudo-labeling layer is trained with ADAM [38], learning

343 rate of 0.001, mini-batch of 10 and an average of 5 epochs at each inner-loop. We experimented with
 344 other possibilities of pseudo-labeler such as a 1-layer perceptron but obtained marginal performance
 345 gain. Baselines’ ER and PseudoER long term classification head are implemented as a one layer
 346 perceptron of size 4096 (also tested variations with marginal variations in results). The ER/PseudoER
 347 replay buffer is set to a size 5000 deep-embeddings for Plants [24], Imagenet21K-OOD [22] and
 348 2500 for eurosat and cifar100. We use a fixed-size memory buffer B_t with the same building strategy
 349 and training loss as in [39]: a buffer of fixed size and prioritizing homogeneous distribution among
 350 classes. That is, an equivalent number of samples of each class are removed if room is required for
 351 new classes and the buffer is full. Equal weight is given to old and new classes during ER. Lastly,
 352 baselines incDFM [11] and DFM [14] were trained using same hyper-parameters proposed by the
 353 authors and their open-source code.

354 4.2.2 Datasets:

355 Since the employed large/foundation feature extractor were pretrained on Imagenet1K, we evaluate
 356 CONCLAD on datasets that either do not contain class overlap with Imagenet1K (out-of-distribution
 357 w.r.t Imagenet1K [40]), or curated them by excluding any overlapping classes. The exception is
 358 cifar100, which was included due to it being a very popular and widespread dataset, also used in
 359 incDFM [11].

- 360 1. *Imagenet21K-OOD (Im21K-OOD)* [22]: We curated a subset of Imagenet21K containing the
 361 top-most populous 50 classes and that do not overlap with the classes present in Imagenet1K.
 362 We use a random set of 500 samples from each of the 50 classes. Because Imagenet21K is a
 363 superset of Imagenet1K, by excluding any overlapping class we guarantee orthogonality
 364 in our curated subset. We will release the full list of images chosen in this curation for
 365 reproducibility.
- 366 2. *iNaturalist-Plants-20 (Plants)* [24]: is a curated subset containing images from 20 OOD
 367 plant species, sourced from the iNaturalist project [24]. A super-set (larger) version of this
 368 subset was originally proposed by [huang2021mos] and has since been frequently used
 369 as test OOD dataset with respect to Imagenet1K [xia2022usefulness, ming2022delving].
 370 Note that we use only 20 classes instead of the original 110 in the [huang2021mos] super-set
 371 since we remove classes with sample count below 140.
- 372 3. *Eurosat* [23]: An RGB dataset of 10 classes and 27K images of Sentinel-2 satellite images,
 373 which is also orthogonal to Imagenet1K.
- 374 4. *Cifar100-Superclasses (Cifar100)* [25]: We use the super-label granularity of Cifar100
 375 dataset. This totals 20 labels (super) and 50K images. While Cifar100 is not orthogonal to
 376 Imagenet1K, we decided to showcase its results since it is a widespread dataset in CL.

377 4.2.3 Baselines

378 For continual novelty detection (CND), we include unsupervised baselines that also utilize FRE-based
 379 uncertainty measures: DFM [26] and incDFM [11]. The latter, incDFM [11], was the first to develop
 380 an updatable continual novelty detector for CND, albeit exclusively tested for the trivialized case of
 381 single class novelties only, see discussion in main paper section 1. Alternatively, DFM originally
 382 introduced the FRE measure 3 for static novelty detection. In the case of incDFM, their proposed
 383 scoring function after training/update could be directly used to compute novelty detection on a test set,
 384 in the continual setting. We use the author’s official implementation of incDFM to generate results.
 385 For DFM, we adapted the method to the continual setting by storing one PCA transform \mathcal{T}_j per task
 386 trained from all data predicted as novel at the previous task. The scoring function S_{DFM}^t for DFM is
 387 defined in equation 4, with T_{old}^t representing the count of how many past tasks with novelty(ies) have
 388 previously occurred at time/task t .

$$S_{DFM}^t(u) = \min_{j \in T_{old}^t} FRE_j(u) \quad (4)$$

389 We also include semi-supervised baselines, with the same tiny supervision budget: (2) ER [27, 6],
 390 originally proposed for supervised CL is adapted to only use actively labeled samples (as embeddings)
 391 for replay; (3) We also adapt PseudoER [29] similar to ER but further incorporating pseudo-labeling of
 392 high confidence unlabeled samples for training. In both ER and PseudoER, we utilize the cumulative
 393 classification entropy as an uncertainty score to actively-label and Pseudo-Label (PseudoER). Similar

394 to CONCLAD, we actively label "ambiguous" samples according to the same formula as outlined
 395 in appendix 4.1.2 for superior results, then sampling according to the TOP heuristic (see section 3
 396 discussion). We also tested with other common uncertainty metrics such as margin [41] but with
 397 inferior results.

398 4.3 Additional Results

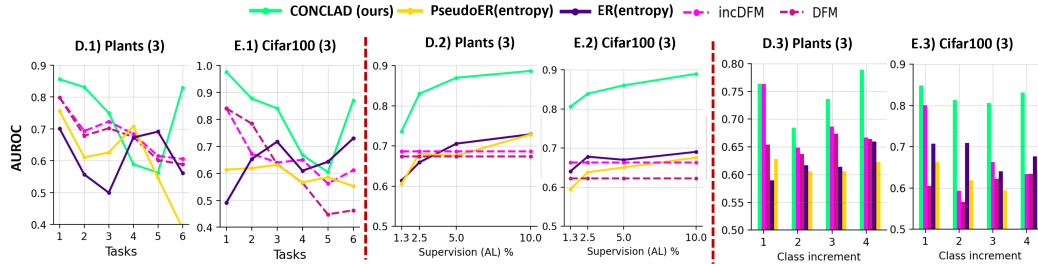


Figure 3: Results for Plants and Cifar100; (Left D.1,E.1) Continual Novelty Detection performance measured by AUROC at each task. The number of novel classes introduced per task is in parenthesis.(Center D.2,E.2) Results varying the supervision budget; (Right D.3,E.3) Results varying Novel Class Increment per task. For (left,right) Supervision budget is 1.25% for CONCLAD, ER, PseudoER. Overall, CONCLAD (green) significantly over-performs baselines